# Practical Methods for Predicting Aerodynamic Heating Effects on Sounding Rockets

L. D. WING*
*NASA Goddard Space Flight Center, Greenbelt, Md.*

**Practical methods for the evaluation of aerothermal effects on sounding rockets need not involve complex exact solutions of the basic physical equations. A collection of four such approximate methods, programed for the IBM 360/91 system, are presented and the validity of their use is demonstrated by a comparison of the theoretical predictions with measurements taken on several sounding rocket flights. Programs 1 and 2 provide means of determining the heat-transfer rates on, respectively, blunt (detached shock wave) and sharp nosed (attached shock wave) bodies in two-dimensional or axisymmetric flow. Programs 3 and 4 utilize the heat rates from the first two programs to derive temperature histories under the assumptions of one- and two-dimensional heat flow, respectively, within the structure.**

## Introduction

EVER since hypersonic flight became a reality for both manned vehicles and unmanned vehicles carrying sensitive payloads, a considerable effort has been expended on theoretical and experimental investigations of the magnitude and effects of aerodynamic heating. A great many purely theoretical, semiempirical and empirical methods have been developed. These methods have varied widely in the degrees of approximation employed.

The most exact methods for solving aerothermodynamic problems would include such ambitious digital computer programs as a three-dimensional method of characteristics, solution of the complete boundary-layer equations, a three-dimensional structural heating program, and some method of handling the complex thermal balance associated with structural cooling and vehicle thermal control systems. At the other extreme, the literature offers a number of semiempirical or empirical techniques that are at once quick, easy to apply, require little or no specialized input and yield results which are adequate for many engineering applications. An attempt is made here to consider the applicability of a few comparatively simple analytical procedures that fall somewhere between these two extremes. It must be emphasized, however, that the greater the degree of approximation in an analytical process, the more sophisticated must be the user's understanding of the subject.

## Summary of Analytical Methods

It is not the purpose here to discuss the analytical methods in great detail or to attempt to consider derivations. The basic theory sources are well-known and are given in the references. The methods of application are discussed in the digital computer program reports cited. Where unpublished work is used, the theory is summarized in the appropriate digital computer program report. Finally, those methods that are felt to be other than very commonly known programing procedures are treated separately in the appendices of the program reports.

Basically, the four programs discussed here provide the design engineer with sufficient analytic capability to handle the vast majority of tasks that arise in the aerothermal design of sounding rockets. Two of the programs are used to derive the boundary-layer to body heat-transfer rates. The other two programs convert these heat rates into temperature histories for particular structural configurations.

### Program 1—The Blunt Body

Program 1 (Ref. 1) has as its primary function the determination of laminar and turbulent boundary-layer aerodynamic heating, friction coefficients, and wall shear stresses along surface streamlines of blunt axisymmetric or two-dimensional bodies (Fig. 1). Capabilities for treating downstream portions (where nose bluntness entropy effects have been dissipated) and swept leading edges (laminar flow only) are incorporated in the program. One streamline cut along the body (up to 50 stations on this cut) and one point in time constitute a run.

Although the program is designed for two-dimensional or axisymmetric bodies only, with it the experienced aerothermodynamicist can make surprisingly good estimates of surface streamline heat-transfer-rate distributions on nonaxisymmetric vehicles or axisymmetric vehicles at angle of attack. Judicious selection of some effective angle of attack at which to switch from the axisymmetric assumption (tangential flow predominates) to the crossflow assumption (tangential flow ignored) is usually based upon some experi-

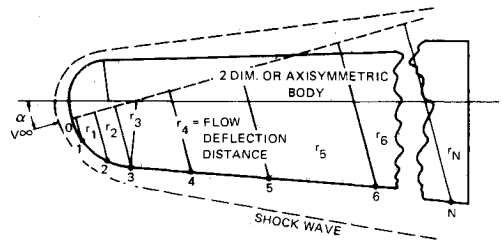


| ITEM | THEORETICAL METHOD | SOURCE |
|---|---|---|
| LAMINAR BOUNDARY LAYER HEAT TRANSFER RATE | ECKERT AND TEWFIK'S REFERENCE ENTHALPY ADAPTATION OF LEE'S INTEGRAL EQUATION | REF. 2 |
| TURBULENT BOUNDARY LAYER HEAT TRANSFER RATE | FLAT PLATE REFERENCE ENTHALPY METHOD | SEE REF. 3 FOR OTHER REFS. |
| STAGNATION POINT HEAT TRANSFER RATE | FAY AND RIDDELL EQUATION | REF.4 |
| HIGH TEMPERATURE AIR PROPERTIES | HANSEN'S APPROXIMATIONS | REF. 5 |

STATION 0 IS THE STAGNATION POINT
STATIONS 1 THROUGH N ARE ARBITRARILY SELECTED LOCATIONS AT WHICH LOCAL PRESSURES ARE INPUT AND HEAT RATES AND SHEAR DATA ARE OUTPUT

**Fig. 1 Program 1, blunt body heating.[1]**

Presented as Paper 70-1399 at the AIAA 2nd Sounding Rocket Technology Conference, Williamsburg, Va, December 7–9, 1970; submitted December 7, 1970; revision received July 8, 1971.
Index category: Rocket Vehicle Aerodynamic Heating.
* Aerospace Engineer. Member AIAA.

mental evidence from either the shape of interest or one that is felt to be sufficiently like it. Thus, the approximate use of the program to cover a three-dimensional case is seen to entail a strong element of empiricism. The blunt-body program is used whenever the vehicle region being investigated is near enough to the separated nose shock wave to be influenced by the high-entropy jump across the normal shock.

### Program 2—The Cone-Cone, Wedge-Wedge Aeroheating Program

Program 2 (Ref. 6) is designed to handle the case of a vehicle having a sharp-nosed conical section that is followed by a conical section of lesser half-angle (Fig. 2). The effects of crossflow arising from low to medium angles of attack (30–40°) are included. The output consists of heat rate and wall-shear stress profiles along the windward generator. The user may elect that the pressure on the downstream cone be derived as the asymptotic cone pressure (the pressure that would exist if the entire body consisted of a cone of the aft-cone half-angle at the appropriate angle of attack) or as the pressure resulting from a real-gas-in-equilibrium, Prandtl-Meyer expansion from the fore body to the aft body. This option exists for either the cone-cone or the wedge-wedge body. The output of the wedge-wedge case is analogous to the cone-cone problem, but there is, of course, no crossflow effect.

In the cone-cone case, the angle of attack is specifically accounted for up to a cone half-angle plus angle of attack of about 40°. Note that if this angle becomes appreciably greater than 40°, the problem ceases to be an attached-shock case. The crossflow then dominates the flow, and the problem becomes more nearly analogous to a blunt body because the body shock will become detached at all stations save the immediate region of the sharp nose tip, which cannot be analyzed by the methods presented in this paper. As is the case with most highly simplified analyses, there is, unfortunately, a region of angle of attack in which it is not clear whether to use the blunt-body program's two-dimensional analysis (Program 1) on the assumption that the heating will be completely dominated by the crossflow or to use the cone-cone analysis (Program 2) with some relatively large angle of attack.

### Program 3–10-Element, One-Dimensional Structural Heating Program

Program 3 (Ref. 10) calculates temperature histories of each element in a 10-element structure consisting of up to 10 materials. The thermal-energy balance is based upon one-dimensional heat transfer. The applicable material densities, coefficients of thermal conductivity, specific heats, and emissivities are inputs. The input heat-rate history can be cold wall, hot wall, or net heat into element 1 (the exposed surface element). If cold-wall heat rates are entered, they are corrected to hot-wall values by the program, which accounts for the enthalpy ratio (though it ignores the cold- to hot-wall heat-transfer coefficient ratio). There are two versions of this program (NZLDW012 and NZLDW017). The former postulates a nonablating surface, and the latter allows for surface recession by using input data that is given either as an effective heat of ablation or as a surface recession rate as a function of heat rate into the structure.

Once again, one sees the use of approximations of the real conditions to obtain design data. It is evident that the thermostructural configuration shown in Fig. 3 can be used to approximate quite reasonably numerous problems whose exact solutions would involve extremely different models. In regions of negligible pressure gradient (e.g., flat plate, cone), the heat transfer rate varies inversely with either the 0.5 (laminar boundary layer) or the 0.2 (turbulent boundary layer) power of the distance along a streamline. Over much of a rocket body, then, it is seen that this relatively small gradient in heat-rate distribution in contiguous surface elements results in only negligible heat flow in the direction parallel to the exposed surface. Therefore, a large number of locations on a typical sounding rocket can be adequately analyzed with the one-dimensional heat-flow assumption. This program can also be used in regions of moderate change of heat rate with distance normal to the primary heat flow if the structure material has a relatively low coefficient of thermal conductivity. In the case of very low-conductivity materials, the program can even be stretched to the ablating stagnation region of a fin (wing) leading edge or a blunted nose.

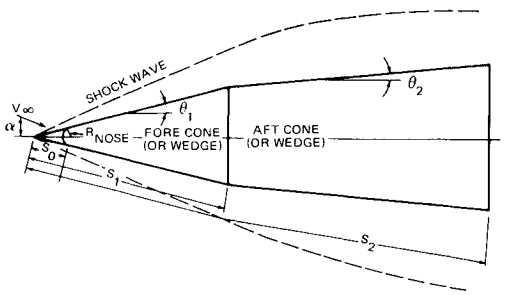


| ITEM | THEORETICAL METHOD | SOURCE |
|---|---|---|
| LAMINAR BOUNDARY LAYER HEAT TRANSFER RATE | ECKERT AND TEWFIK'S REFERENCE ENTHALPY ADAPTATION OF LEE'S INTEGRAL EQUATION (REDUCED TO CONSTANT PRESSURE CASE) | REF. 2 |
| TURBULENT BOUNDARY LAYER HEAT TRANSFER RATE | FLAT PLATE REFERENCE ENTHALPY METHOD | REFS. 3, 7, 8 AND 9 |
| CROSS-FLOW EFFECTS IN LAMINAR AND TURBULENT BOUNDARY LAYERS | DEVELOPMENTS OF THESE METHODS ARE SHOWN IN THE PROGRAM REPORT | REF. 6 |
| HIGH TEMPERATURE AIR PROPERTIES | HANSEN'S APPROXIMATIONS | REF. 5 |

**Fig. 2 Program 2, cone-cone or wedge-wedge heating.[6]**

### Program 4—28-Element, Two-Dimensional Structural Heating Program

Program 4 (Ref. 11) is similar to the one-dimensional program just described (Program 3) except that it analyzes a 28-

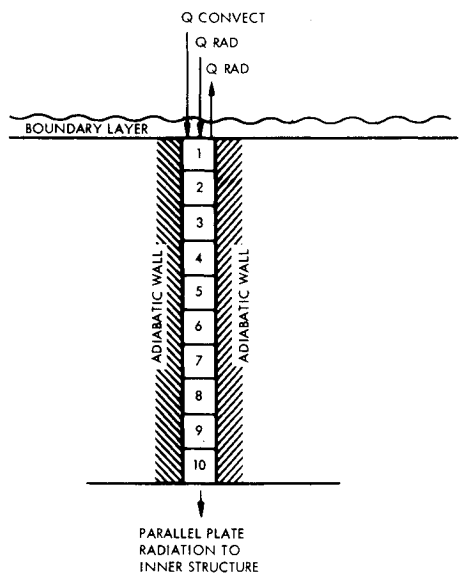


| ITEM | THEORETICAL METHOD | SOURCE |
|---|---|---|
| TEMPERATURE HISTORIES OF EACH OF THE 10 ELEMENTS | SIMULTANEOUS SOLUTION OF THE TEN HEAT BALANCE EQUATIONS | REF. 10 |

**Fig. 3 Program 3, 10-element, one-dimensional structural heating.[10]**

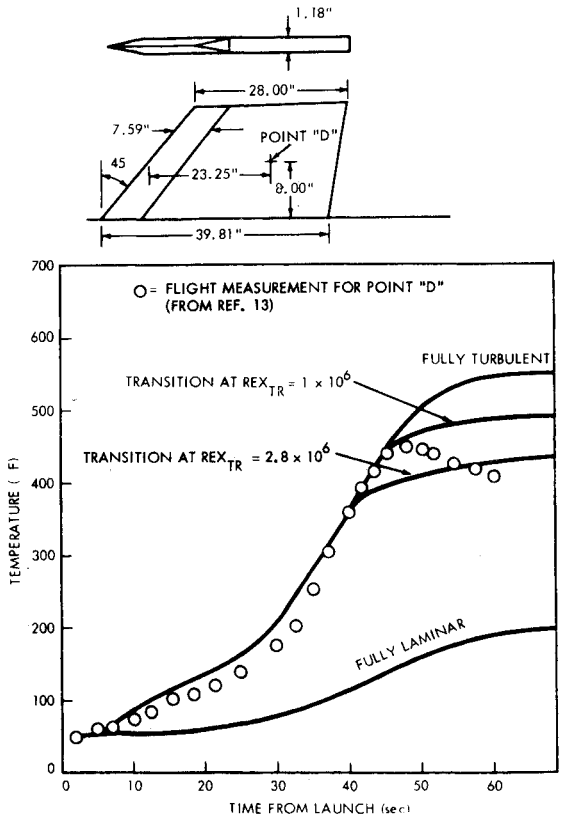


**Fig. 4 Aerobee 150A, flight 4.12. Theoretical and flight-recorded temperature comparisons on fin-point "D."**

element network structure. Elements 1–7 are exposed to a boundary layer or other heat source, and elements 22–28 are either exposed to cooling by parallel-plate radiation to some inner vehicle structure or they are adiabatic on their exposed (inner) surfaces. The dimensions of the elements can be input individually to achieve various overall structural shapes, but the contiguity of the elements is fixed; that is, element 1 is always bordered by elements 2 and 8, etc. The program is specifically designed to handle the case of a fin, a wing leading edge, or an axisymmetric nose at a very low angle of attack and which is constructed of a high-conductivity material but which has a steep surface heat-transfer-rate gradient.

The theory consists of the simultaneous solution of 28 heat-balance equations.[11] As in Program 3, each element can be made of any material. The emissivities of the exposed elements (1–7) can be input as constants or as linear or second-order variables with surface temperature. All material specific heats and thermal conductivities can be given as constants or linear variables with temperature.

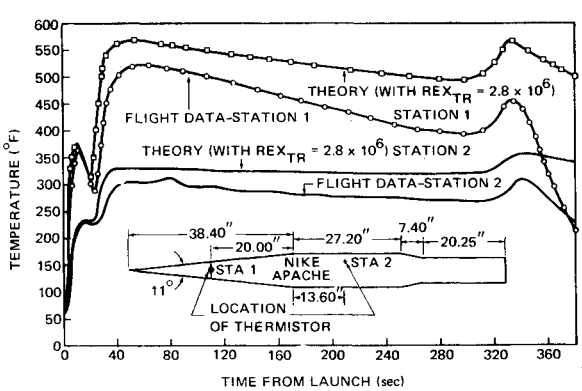


**Fig. 5 Nike Apache, flight 14.363 GT. Comparison of flight data with theory at stations 1 and 2.**

## Discussion

Over a period of several years, the methods of Programs 1 and 2 have been used to predict heat-transfer-rate distributions on numerous body shapes that have been subsequently tested in various wind tunnels. The agreement between theory and experiment has been reasonable, in general, even with such complex shapes as the SV-5 re-entry vehicle over a wide range of angles of attack. An earlier (perfect gas) version of Program 2 was used with satisfactory results to predict heating on a very-high-performance air-defense missile. In this context, it is the author's viewpoint that any aerodynamic heating analysis that can consistently predict heat-transfer rates within 20% is indeed an excellent method. In the case of asymmetric vehicles, this figure would probably lie between 50 and 100%. Inasmuch as mismatching of Reynolds and local Mach numbers, scale factor problems and absence of real gas effects tend to complicate evaluation of theory by means of wind tunnel data, only comparisons of temperatures obtained by the methods of Programs 1–4 with flight data from sounding rocket flights are presented.

### Quality of Flight Measurements

The random nature of flight data available for these examples is ample testimony to the need for more and better flight measurements. A significant proportion of the data are obtained from instrumentation that has been added at the last minute on an available telemetry space basis. Often thermistors are used (when better measurements could be made with other instrumentation) simply to conserve telemetry space. Finally, the resulting isolated temperature sensor locations make it virtually impossible to establish heat rate distributions or to locate possible hot spots deriving from (e.g.) shock-wave boundary-layer interactions.

### Transition Criteria

The extremely large amount of theoretical and experimental work that has been done on the subject of transition Reynolds numbers has led to the adoption of numerous criteria. It is most convenient (at the sacrifice of accuracy, of course) to adopt some magic numbers that one hopes will yield reasonable results over a wide range of cases. The author has quite arbitrarily selected the following criteria for use whenever experimental data for the specific case are not available: 1) transition from laminar to turbulent flow takes place whenever the local Reynolds number ($Re\chi_{TR}$) exceeds 2.8 million for all zero (or very-low) pressure-gradient cases; 2) in the regions of noses or leading edges where the pressure gradients are appreciable, transition from laminar to turbulent flow is assumed to occur at a momentum-thickness Reynolds number ($Re\theta_{TR}$) of 250.

In the special case where a point on an ogive nose is being analyzed by means of the cone-cylinder option of Program 2, present experience indicates that an effective local Reynolds number at transition value is approximately 15–20 million. This value may be modified in cases where experimental evidence is available or as additional experimental data are accumulated. Of course, this criterion, in common with the cone-cylinder simulation, is valid only for ogives that are sufficiently slender to maintain an attached nose shock. Note, however, that Rumsey and Lee[12] show transition Reynolds numbers varying between 14.2 and 30.3 million on a slender cone.

A small amount of data shows transition occurring at Reynolds numbers below these values, but, in general, the numbers given are conservatively low. It must be remembered that the phenomenon of transition is very complex and has been shown to be dependent upon a large number of variables. Even more conservative values found in the literature for the transition Reynolds numbers are $Re\chi_{TR} = 1 \times 10^6$; $Re\theta_{TR} =$ 150 to 200. In the final analysis, the individual engineer

must sift the available data that most closely approach the case of interest and decide for himself what criteria to adopt.

### Sample Cases

The following cases compare the theoretical calculations of Programs 1–3 with specific flight cases that involve only sounding rockets. These cases have been screened in the sense that no flight data have been used if obvious anomalies were found. Such anomalies usually result from some form of system failure (telemetry blackout, temperature-sensor failure, etc.), so their inclusion would be meaningless.

#### *Case 1—Aerobee 150A fin*

A point 2 ft aft of the leading edge and 8 in. outboard of the root chord on the Aerobee 150A fin (flight 4.12 GT) has been examined theoretically, and a comparison has been made with the flight-measured data.[13] The structural configuration, a swept-back wedge leading-edge fin, is shown in Fig. 4. Point *D* is located on the 0.05-in. magnesium skin of the fin. The heat-transfer rate is calculated with the two-dimensional option of Program 2. The pressure on the flat plate is obtained by assuming a Prandtl-Meyer expansion from the wedge leading edge. The transition Reynolds number is taken as 2.8 million. The temperature history at point *D* is obtained from the above heat rates in conjunction with Program 3, the 10-element, one-dimensional structural heating program. Point *D* is fairly well isolated thermally on the magnesium skin; that is, there are no significant heat masses within 2 in. of point *D*.

The solid lines on Fig. 4 represent the theoretical temperature histories with the assumptions of (from top to bottom) a fully turbulent boundary layer, a transition at a local Reynolds number of 1 million, a transition at a local Reynolds number of 2.8 million, and a fully laminar boundary layer. The general correlation in this case is seen to be good—on the comfortably conservative side. However, it appears that transition from turbulent to laminar flow occurred at a local Reynolds number that was closer to 1 million than to 2.8 million. The steeper slope of the experimental-data curve in the cooling region (after 48 sec) is very frequently observed in flight data. It is probably caused by the effects of conduction parallel to the exposed surface (not accounted for in the theory of Program 3), which are most significant during periods of very low or even negative heat-transfer rates.

#### *Case II—Nike Apache nose cone*

A point approximately 1.5 ft aft of the nose-cone apex on the Nike Apache (flight 14.363 GT) nose has been used to compare flight temperature data with the theoretical predictions of Programs 1–3 (Ref. 14). In this case, the conical-flow option of Program 2 is used through ascent, and the two-dimensional option of Program 1 is used during re-entry. The vehicle angle of attack through ascent is approximately zero. No attitude measurements were taken during re-entry, but the use of theoretical trajectory analysis to match the flight-recorded altitude and velocity histories through re-entry indicated that the re-entry angle of attack was very close to 90°. The re-entry heat-rate curve is also reduced by a factor of 0.377 to account for the fact that the body is spinning at a rate in excess of 1 cycle/sec. Thus, for the re-entry portion, Program 1 is used because it is assumed that the crossflow predominates and that the tangential flow can be ignored. Once the ascent, out-of-atmosphere (cooling), and re-entry heat-rate histories are established, Program 3 is used to determine the temperature history of the 0.083 in. (thermally-isolated) aluminum skin.

Figure 5 presents the theoretical and flight-measured temperature histories at station 1 and station 2 along with a sketch of the vehicle that shows the location of the two points investigated. Once again, if the transition Reynolds number

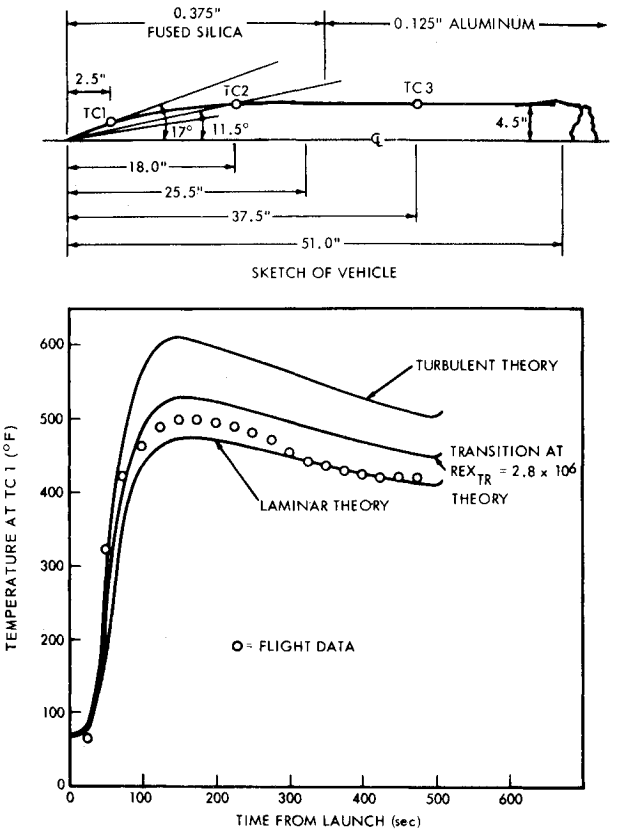


**Fig. 6 Nike Tomahawk, flight 18.08 GE. Comparison of flight-temperature data at TC 1 with theory. Inner surface of 0.375-in. fused silica.**

is assumed to be 2.8 million, the agreement is quite reasonable. The only anomaly occurs during the latter part of re-entry—the characteristic steep negative slopes of the flight-temperature curves of Fig. 5. No very convincing explanation was found for this rapid cooling, so, as in Case I, it was assumed that horizontal conduction must be involved.

#### *Case III—Nike Tomahawk flight 18.08 GE*

In Nike Tomahawk Flight 18.08 GE (Ref. 15) two temperature measurements are considered on the inner surface of the 0.375-in. slip-cast fused-silica ogive nose, and one on the inner surface of the 0.25-in. aluminum, cylindrical payload section. The vehicle geometry and the location of the heating points are shown in Fig. 6. The theoretical analyses were made with Programs 2 and 3. In order to approximate the ogive shape by means of the cone-cone option of Program 2, the

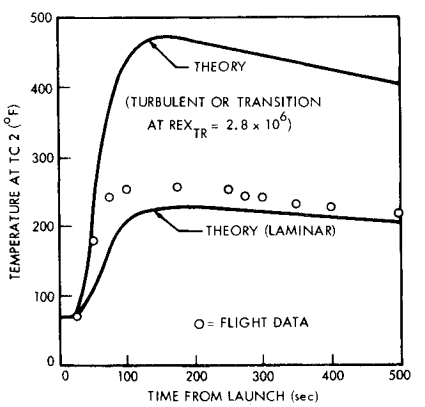


**Fig. 7 Nike Tomahawk, flight 18.08 GE. Comparison of flight-temperature data at TC 2 with theory. Inner surface of 0.375-in. fused silica.**

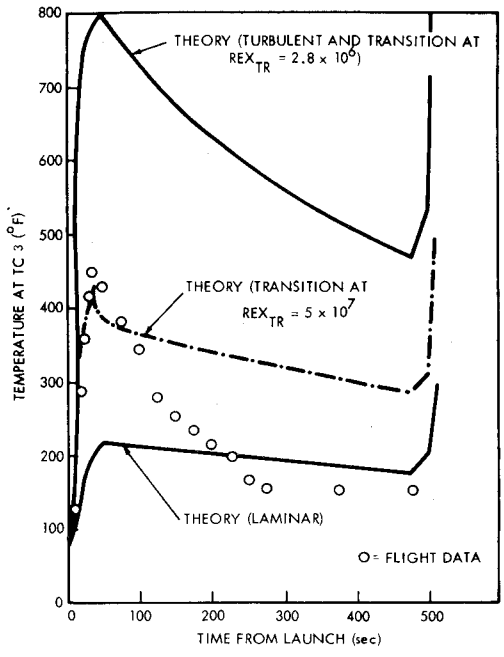


**Fig. 8 Nike Tomahawk, flight 18.08 GE. Comparison of flight-temperature data at TC 3 with theory. Inner surface of 0.125-in. aluminum sheet.**

assumption is made that points TC1 and TC2 are located on two tandem conic sections. The fore conic section has a 17.5° half-angle, and the aft conic section has an 11.5° half angle. The appropriate boundary-layer buildup distances to these two points are used. For point TC3, a fore cone (10° half-angle) is correctly assumed to be followed by a cylindrical body on which TC3 is located.

The heat-transfer-rate histories from Program 2 are input into Program 3 (the one-dimensional structural heating program), and the data of Figs. 6–8 result. The flight data are shown as circled points on these figures. The data for TC1 and TC2 (measurements taken on the inner surface of the 0.375-in. fused-silica nose) show quite good correlation with the laminar theory throughout, despite the fact that at TC2, the local Reynolds numbers greatly exceed the commonly used transition values of 1–3 million.

The point farther down the vehicle, TC3, appears to have experienced transition at approximately 15 sec into the flight. This would indicate a transition Reynolds number of as much as 50 million. This method of predicting transition Reynolds numbers is crude at best, so one can only estimate the actual value as somewhere between 10 and 50 million. The significant point is that, throughout this flight, extremely high indicated local Reynolds numbers are reached at times when the flight-temperature data match the laminar theoretical predictions very well (see also Case IV and Rumsey and Lee's work[12]).

The dashed curve of Fig. 8 results (Ref. 12) from using the transition time in flight to infer the point at which the local boundary layer passes from turbulent to laminar (15 sec) and rerunning the structural heating program with the appropriate changes in the boundary layer to wall heat rates. This first-cut correction succeeds in matching the flight-temperature curve at TC3 quite well during the significant aerodynamic-heating portion of flight. The very steep slope of the flight-temperature curve for TC3 does not match the theory at all. This discrepancy arises from the fact that TC3 is in the high-conductivity-material region and, when the heat rates from the boundary layer become small, the one-dimensional assumption for the structural heating becomes invalid. The heat conduction parallel to the aluminum surface becomes large with respect to the heat passing through the exposed

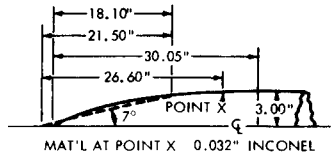


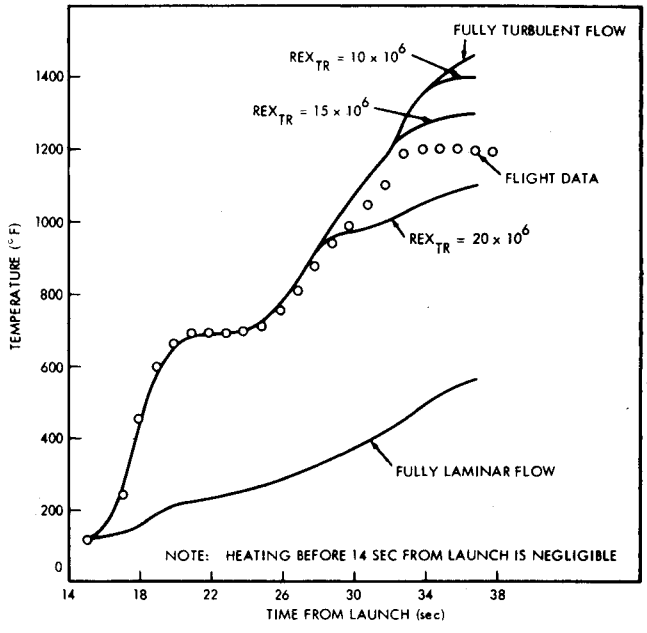


**Fig. 9 Four-stage vehicle with ogive nose. Flight-temperature at point $\chi$ compared with theory.**

surface of the wall. Notice that, at TC1 and TC2 the slopes for theory and flight are matched much better through the out-of-atmosphere region because the fused silica has a low coefficient of thermal conductivity.

In summary, the comparison of the data in general is good. The weakness of the one-dimensional structural-heating assumption for high-conductivity materials in low heat-transfer portions of flight is demonstrated. Finally, the facts that the fused silica is exceptionally smooth surfaced, that the ogive nose results in nonzero pressure gradients along surface streamlines, and that the local Mach numbers calculated are relatively high all contribute to extremely high (apparent) transition Reynolds numbers.

### *Case IV—Four stage test vehicle with ogive nose*

A four-stage rocket propelled the nose configuration shown in Fig. 12 to a Mach number of 10.4 (Ref. 16). Temperature measurements were made on the inner surface of the 0.032-in. inconel ogive at point $\chi$. These temperature data are shown as circled dots in Fig. 9.

As with the ogive nose problem of Case III, the cone-cylinder option of Program 2 was used to simulate the ogive shape. In this case, a 7° cone followed by a cylinder was used, with the assumption that point $\chi$ lay on the cylinder. The heat-transfer rate data so obtained was fed into Program 3, which gave the theoretical curves (solid lines) of Fig. 9. This study has been reported in detail by the author.[17]

The agreement between flight data and the turbulent boundary-layer calculation is very good up to about 28 sec. Somewhere within the next 10 sec, the boundary layer commences transition to laminar flow. The Reynolds number for transition, deduced from the location of the flight-data curve of Fig. 9, is between 15 and 20 million (probably closer to 15 million). According to Bland and Collie,[16] transition occurs at a local Reynolds number of about 6.8 million, or

only about half the value indicated by this author.[17] This apparent discrepancy is believed to result from the manner in which the real geometry is approximated. It has already been poined out that the transition Reynolds number on an ogive should be larger than that of a cone under similar flight and surface conditions because of the pressure-gradient effect. This accounts for Bland and Collie's[16] value of 6.8 million instead of the present paper's value of 2.8 million for cones or flat plates. Under the conditions of Cases III and IV, there is an additional increase that arises from the fact that the real pressure on the ogive at point $\chi$ is somewhere between the post-oblique nose shock and the freestream values. In the cone-cylinder approximation, the pressure is given as the freestream value at point $\chi$. This overexpansion results in local Mach numbers that are higher in the theoretical case than those reported by Bland and Collie.[16] Thus, the 15–20-million value of local Reynolds number at transition is valid only when one restricts its application to the geometry-simulation method used here. For this reason, the term "effective Reynolds number of transition" is used to describe the 20 million value.

## Conclusions

The analytical methods and flight-data substantiation presented in this paper have led to the following three conclusions:

1) The lack of man-rating, comparatively low sensitivity to thermal-protection system weight, generally less accurate trajectory requirements and the low cost of sounding rockets result in the justification of something less than the most accurate (and expensive) analytical design methods. However, more extensive and better quality flight temperature measurements would be very helpful in perfecting the application of the methods described.

2) The analytical capability represented by the four digital programs discussed should yield structural-temperature predictions that are within 20–25% of the conditions that will exist in flight. In general, the predictions will be conservatively high.

3) For the analytical methods of Programs 1 and 2, the following local Reynolds numbers have been found to be reasonable approximations for the transition from laminar to turbulent flow: a) for cases of zero pressure gradient along streamlines, the local transition Reynolds number is approximately 2.8 million; b) For cases having a steep pressure gradient (blunt bodies), the local momentum-thickness Reynolds number is approximately 200–250; c) For slender ogive noses (bow shock attached) approximated by the cone-cone or cone-cylinder options of Program 2, the effective local transition Reynolds number (the value calculated by the program) is of the order of 15 million.

Note that no detailed measurements of fin leading-edge (two-dimensional) temperature distributions have been made, and, therefore, this paper does not discuss any flight test of the capability of Program 4. However, Program 4 has been compared with a Langley Research Center general two-dimensional, non-ablative structural heating program (LRC identification: D1244), and agreement was found to be within less than 1%.

## References


[1] Wing, L. D., "General Aerodynamic Heating—Blunt Body Aeroheating Digital Computer Program NZLDW001," Rept. ER 109, Oct. 1967, Technical Services Div., Fairchild Hiller Corp., Riverdale, Md.

[2] Eckert, E. R. G. and Tewfik, O. E., "Use of Reference Enthalpy in Specifying the Laminar Heat Transfer Distribution Around Blunt Bodies in Dissociated Air," *Journal of the Aerospace Sciences*, Vol. 27, No. 6, June 1960, p. 464.

[3] Libby, P. A. and Cresci, R. J., "Evaluation of Several Hypersonic Turbulent Heat Transfer Analyses by Comparison with Experimental Data," TN-57-72, AD118093, July 1957, Wright Air Development Center, Wright-Patterson Air Force Base, Ohio.

[4] Fay, J. A. and Riddell, F. R., "Theory of Stagnation Point Heat Transfer in Dissociated Air," *Journal of the Aerospace Sciences*, Vol. 25, No. 2, Feb. 1958, p. 73.

[5] Hansen, C. F., "Approximations for the Thermodynamic and Transport Properties of High Temperature Air," TR-R50, 1959, NASA.

[6] Wing, L. D., "Aerodynamic Heating for Wedge/Wedge or Cone/Cone at Angles of Attack from Zero to Approximately 40°—Digital Computer Program NZLDW005," Rept. ER 116, Nov. 1968, Technical Services Div., Fairchild Hiller Corp., Riverdale, Md.

[7] Cresci, R. J., MacKenzie, D. A., and Libby, P. A., "An Investigation of Laminar, Transitional and Turbulent Heat Transfer Rate on Blunt Nosed Bodies in Hypersonic Flow." *Journal of the Aerospace Sciences*, Vol. 27, No. 6, June 1960, p. 401.

[8] Zakkay, V. and Callahan, C. J., "Laminar, Transitional and Turbulent Heat Transfer to a Cone-Cylinder-Flare Body at Mach 8," PIBAL Rept. 737 (AFOSR2359), Feb. 1962, Polytechnic Institute of Brooklyn, Brooklyn, New York.

[9] Eckert, E. R. G., "Survey on Heat Transfer at High Speeds," TR-54-70, April 1954, Wright Air Development Center, Wright-Patterson Air Force Base, Ohio.

[10] Wing, L. D., "10-Element, One Dimensional Structural Heating Programs," GSFC X-721-69-454, 1969, NASA.

[11] Wing, L. D., "A 28-Element, Two Dimensional Structural Heating Program (NZLDW018)," GSFC X-721-70-221, 1970, NASA.

[12] Rumsey, C. B. and Lee, D. B., "Measurements of Aerodynamic Heat Transfer and Boundary Layer Transition on a 15° Cone in Free Flight at Supersonic Mach Numbers up to 5.2," TN-D888, Aug. 1961, NASA.

[13] Wing, L. D. and Bensimon, M., "Analysis of Aeroheating and Loads on Fins of Aerobee 150A and 170," GSFC X-721-69-473, 1969, NASA.

[14] Crawford, L. W., "Comparison of Analytical and Flight Recorded Temperature Histories for Nike Apache Flight 14.363 GT," U.S. Government Memorandum to Flight Performance Section Files, Oct. 29, 1969.

[15] Wing, L. D., "Comparison of Theoretical Predictions with Flight Recorded Temperatures on Nike Tomahawk Flight 18.08 GE," U.S. Government Memorandum to Flight Performance Section Files, April 8, 1970.

[16] Bland, W. M. and Collie, K. A., "Free Flight Aerodynamic Heating Data to Mach Number 10.4 for a Modified Von Kármán Nose Shape," TN-D889, May 1961, NASA.

[17] Wing, L. D., "Comparison of Flight Performance Section Aerodynamic Heating Analytical Methods with Flight Data from NASA TN-D889," U.S. Government Memorandum to Flight Performance Section Files, April 29, 1970.